Plant Soil (2026) 525:145–161
https://doi.org/10.1007/s11104-025-07445-z

RESEARCH ARTICLE

Acidification associated with plant phosphorus-acquisition strategies decreases nutrient cycling potential of rhizosphere bacteria along the Hailuogou post-glacial chronosequence

Xiao-Long Li · Hongyang Sun · Jun Zhou · Yang Chen · Hong-Qiu Du · Yue-Xin Ming · Shuang Wu · Hans Lambers

Received: 26 November 2024 / Accepted: 4 April 2025 / Published online: 16 April 2025
© The Author(s) 2025

Abstract

Background and aim Soil nutrient availability, acidification associated with plant phosphorus-mining strategies, and fine root foraging all influence nutrient cycling. However, their relative impacts on microbial nutrient cycling during primary succession remain unclear.

Methods We studied a 130-year primary succession along the Hailuogou post-glacial chronosequence in southwest China. Early-successional stages (1–3) are dominated by *Hippophae tibetana*, which is gradually replaced by *Populus purdomii*. In the climax community (stage 4), *Abies fabri* replaces *P. purdomii*. We collected rhizosphere soil, roots, and leaves from the dominant species, analyzing how phosphorus-acquisition strategies (proxied by soil pH, leaf manganese concentration and fine-root morphology) influenced bacterial nutrient-cycling gene abundance, based on 16S rRNA sequencing.

Results Rhizosphere pH and the abundance of genes encoding enzymes involved in ammonium and nitrate assimilation, denitrification and phosphorus mobilization were significantly lower for *H. tibetana* and *A. fabri* than for *P. purdomii*. In contrast, *P. purdomii* exhibited a significantly higher specific root length. Linear mixed models reveal that leaf manganese concentration was positively correlated with soil acidification. Multiple regression models show that nutrient-cycling potential was more significantly linked to soil pH than to fine-root morphology or soil nutrient availability. Structural equation models indicate that the reduced nutrient-cycling potential was indirectly associated with soil acidification through bacterial co-occurrence networks rather than bacterial richness.

Conclusion Soil acidification, associated with phosphorus-mining strategies of *H. tibetana* and *A. fabri*, may inhibit microbial nutrient-cycling potential during primary succession. This highlights the interactions between plant nutrient-acquisition strategies

Responsible Editor: Benjamin L. Turner.

Supplementary Information The online version contains supplementary material available at https://doi.org/10.1007/s11104-025-07445-z.

X.-L. Li · J. Zhou (✉) · Y. Chen · H.-Q. Du · Y.-X. Ming · S. Wu
Institute of Mountain Hazards and Environment, Chinese Academy of Sciences, Chengdu 610299, China
e-mail: zhoujun@imde.ac.cn

H. Sun
Sichuan Zoige Alpine Wetland Ecosystem National Observation and Research Station, Southwest Minzu University, Chengdu 610225, China

H.-Q. Du · Y.-X. Ming · S. Wu
University of Chinese Academy of Sciences, Beijing 101408, China

H. Lambers
School of Biological Sciences and Institute of Agriculture, University of Western Australia, 35 Stirling Highway, Perth, WA 6009, Australia

and microbial processes in shaping terrestrial nutrient cycling.

Keywords Plant-microorganism interaction · Chronosequence · Co-occurrence network · Bacterial diversity · Scavenging strategy

Introduction

Nitrogen (N) and phosphorus (P) are essential nutrients that may limit plant and microbial growth in various ecosystems (Wassen et al. 2005; Lambers et al. 2008). Rapid nutrient cycling plays an important role in supporting the establishment of pioneer plant communities and enhancing vegetation changes during primary succession (Sparrius and Kooijman 2013; Ciccazzo et al. 2016). Soil bacteria are the major microorganisms responsible for a variety of transforming processes of N and P, such as assimilation, mineralization, fixation nitrification and denitrification of N and solubilization and mineralization of P (McGrath et al. 2013; Kuypers et al. 2018). These processes can increase soil nutrient availability and thus enhance nutrient uptake in diverse plants (Cheng et al. 2024). Plants exhibit an array of strategies for nutrient acquisition, such as foraging bioavailable nutrients from soil via extensive fine root systems and mobilize insoluble nutrients via proton and carboxylate release (Lambers 2022). These strategies have the potential to inhibit bacterial nutrient cycling, decreasing the positive impacts of bacteria on plant nutrient uptake (Chapman et al. 2006; Moreau et al. 2019; Prescott et al. 2020). The strategies that plants and bacteria utilize to acquire nutrients vary greatly with plant species replacement and simultaneous soil nutrient availability (Lambers et al. 2008; Zemunik et al. 2015; Ortiz-Álvarez et al. 2018; Turner et al. 2019; Li et al. 2025). However, the extent and mechanisms by which plant nutrient-acquisition strategies impact bacterial nutrient cycling during primary succession remain poorly understood. The aim of this study is to estimate the impacts of interspecific differences in nutrient-acquisition strategies on nutrient cycling potential of rhizosphere bacteria during primary succession.

Soil acidification has the potential to inhibit the activities and composition of soil bacterial communities and thus soil nutrient cycling through allowing soil pH to deviate from optimum values for microorganisms (Kuzyakov and Xu 2013). For example, studies focusing on crops in China show that soil acidification plays a major role in decreasing the abundance of genes encoding enzymes involved in bacterial P solubilization, uptake and transport (Dai et al. 2020). However, a study conducted on tropical acidic soils where most P is sorbed onto iron- and aluminum-bearing minerals shows that soil acidification beneath N_2-fixing plants enhances P cycling as it promotes the growth of soil Fe-reducing bacteria, and in turn increases the solubilization of P (Epihov et al. 2021). Additionally, acidification generally decreases the abundance of genes encoding enzymes involved in nitrification due to the acidification stress on nitrifiers (DeForest and Otuya 2020; Zhou et al. 2023). It likely also decreases the rates of hydrolysis of organic N and assimilation of ammonium N, but it enhances nitrate assimilation (Broadbent and Tyler 1965; Fisher et al. 2017). However, acidification may indirectly, and not directly, impede N assimilation through decreasing nitrate and ammonium N produced from nitrification and mineralization, respectively (Elrys et al. 2022). The strategies that acidify soil are important for successional species growing in young soils with abundant primary mineral P (Zhou et al. 2013), but it remains unclear how acidification associated with plant P-acquisition strategies influences bacterial nutrient cycling during primary succession.

The development of extending fine roots is effective at foraging soluble nutrients from soil (Francis and Read 1994). Fine root foraging may affect the substrate for soil bacteria and thus bacterial nutrient cycling (Moreau et al. 2019). For example, increased N acquisition by grassland species associated with greater root length density decreases the substrate (nitrate–N) for denitrifiers, leading to reduced emission of nitrous oxide (Abalos et al. 2018). Similarly, plants possessing greater specific root length (SRL) and with a high affinity for ammonium N exhibit a lower potential rate of nitrification in a European grassland (Cantarel et al. 2015). However, more rapid N uptake through fine roots may be associated with greater input of labile carbon, thus accelerating N cycling through priming effects (Henneron et al. 2020). Although fine root foraging and acidification are two complementary strategies and often co-occur during primary succession, knowledge on which

of these strategies has a greater impact on bacterial nutrient cycling is still lacking.

Soil microbial diversity is essential to maintain soil nutrient cycling. For example, soil acidification caused by nutrient enrichment indirectly impacts multiple ecosystem functions (e.g., nutrient cycling) through affecting microbial diversity (Hu et al. 2024). A microcosm experiment shows that a 75% decrease in bacterial species richness through serial dilution reduces denitrification potential in soil by 70–80% (Philippot et al. 2013). In addition, plant P-acquisition strategies are likely to influence the abundance of specific microorganisms within modules related to soil nutrient cycling (Wagg et al. 2019). A module is defined as a cluster of highly-interconnected taxa of microbial networks and microbial taxa within an individual module are likely associated with similar nutrient cycling (Bissett et al. 2013). For example, a microbial network composed of bacteria, fungi, and nematodes reveals that different modules are characterized by distinct groups of microorganisms, including those involved in nutrient cycling, putative plant pathogens and arbuscular mycorrhizal fungi (Fan et al. 2021). Similarly, a N addition experiment in a subtropical plantation of Moso bamboo shows that greater bacterial relative abundance within a particular module account for increased phosphatase activities and abundance of genes encoding enzymes associated with P cycling (Zeng et al. 2024). While both richness of bacterial communities and abundance of bacteria belonging to a particular module play important roles in affecting soil nutrient cycling, it is unclear whether plant nutrient-acquisition strategies influence bacterial nutrient cycling through their effects on bacterial diversity and abundance within modules of co-occurrence networks.

The Hailuogou postglacial chronosequence with primary vegetation succession on the eastern edge of the Tibetan Plateau, southwest China is an ideal place to address the above questions. The pioneer plant communities are dominated by *Hippophae tibetana* (Elaeagnaceae) and *Populus purdomii* (Salicaceae), and the climax plant communities are dominated by *Abies fabri* (Pinaceae) along the chronosequence. The actinorhizal (N_2-fixing) *Hippophae* genus forms cluster roots that release large amounts of carboxylates and protons (Shah et al. 2015). Soil acidification caused by actinorhizal plants can even accelerate rock weathering (Perakis and Pett-Ridge 2019). The *Populus* and *Abies* genera forage bioavailable nutrients and may mobilize sparingly-soluble nutrients via ectomycorrhizas (Xia et al. 2020a, b). Thus, acidifying and foraging capacity may differ among the dominant species. Moreover, the potential assimilatory nitrate reduction of bacteria differs among co-occurring plant species at the stage dominated by *H. tibetana* (Sun et al. 2023). Soil pH contributes to a change in the bacterial community associated with the release of alkaline phosphatases along the Hailuogou chronosequence (Bai et al. 2020). We therefore hypothesized that (i) soil acidification decreases the nutrient-cycling potential of rhizosphere bacteria; (ii) acidification has greater impacts on nutrient cycling than fine root foraging does. The objectives of this study were to (i) determine the relative contribution of acidifying and fine root foraging strategies in influencing potential nutrient cycling of rhizosphere bacteria; (ii) determine the direct and indirect impacts of nutrient-acquisition strategies on nutrient cycling though bacterial richness and the abundance of taxa within modules of co-occurrence networks.

Materials and methods

Study area

The Hailuogou Glacier is located on the eastern slope of the Gongga Mountain, straddling the transition zone of the Tibetan Plateau and the Sichuan Basin. A ~ 130-year-old primary succession has developed from bare soil to a climax plant community along the Hailuogou Glacier retreat area. Plant community composition and soil nutrient bioavailability change rapidly during primary succession (Li and Xiong 1995; Zhou et al. 2013). Three stages were chosen to represent the pioneer plant communities. *Hippophae tibetana* is dominant at the S1 stage (8–12 years) and *H. tibetana* and *P. purdomii* dominate at the S2 stage (32–42 years). *Populus purdomii* replaces *H. tibetana* at the S3 stage (50–60 years). The S4 stage (80–90 years) represents the plant community with abundant *A. fabri* and a few *P. purdomii*. The relative coverage of the former is about 85% but that of the latter is 10%. Plant communities establish on fine moraine material at the glacier terminus and S1 stage, while those at the later stage (S2-S4) colonize soil with developing litter layers (Zhou et al. 2019). Although

soil physicochemical properties significantly change with soil age, soil conditions are similar within each stage (Zhou et al. 2013). The entire chronosequence (spanning < 2 km length and 80–200 m width) occurs within a narrow elevational range (2900–2982 m above sea level), ensuring homogeneous microclimate (precipitation and temperature) and topography. The mean annual temperature and precipitation is 4.2℃ and 1947 mm, respectively (Zhou et al. 2013). The mean annual soil temperature at 5 cm depth is 5.8–6.1℃ along the chronosequence (Zhou et al. 2016). The soils are classified as Regosols according to the World Reference Base for Soil Classification (Zhou et al. 2013). The mean concentrations (standard error) of bioavailable soil N (nitrate and ammonium) in mineral horizons are: S1 stage 0.6 (0.2), S2 stage 7.3 (1.1), S3 stage 11.0 (2.0), S4 stage 1.7 (0.7) mg N kg^{-1}. The mean concentrations (standard error) of bioavailable soil P in mineral horizons are: S1 stage 1.8 (0.4), S2 stage 8.4 (1.4), S3 stage 16.1 (3.8), S4 stage 5.3 (1.8) mg P kg^{-1}.

Field sampling

Fine roots (< 2 mm diameter) and soil were collected from five *H. tibetana* and *P. purdomii* individuals at the first three stages (S1–3) and five *P. purdomii* and *A. fabri* individuals in July 2022. Along the primary roots of trees and their branches, we determined the fine roots of target tree species. We collected soil within 2 cm of fine roots of these individuals as rhizosheath-like soil since it is hard to collect enough 'real' rhizosheath soil (< 1 mm adhering to fine roots). To minimize interference from the roots of co-occurring plants, soil samples were collected directly adjacent to the roots of the target tree species, avoiding areas with potential root overlap from other species. Before collecting soil samples, plant litter and any soil adhering to herbaceous roots were carefully removed to reduce the influence of herbs on the rhizosheath-like soil of the target trees. In addition, five replicates of topsoil (0–10 cm deep) were also collected to represent bare soil at the terminal of the glacier. Only fine moraine material was sampled at the terminal of the glacier and S1 stage. Fresh soil samples were sieved and divided into two subsamples, one was stored at 4℃, and the other at − 80℃ for analysis of bacterial community composition.

Soil DNA extraction and PCR amplification

To determine the bacterial community composition associated with N cycling, DNA was extracted from soil samples by using the ALFA-SEQ Advanced Soil DNA Kit (mCHIP, Guangzhou, China). The concentration and purity of the genomic DNA were checked on the NanoDrop One (Thermo Fisher Scientific, Massachusetts, USA). The regions of the 16S rRNA genes for bacteria (V4–V5 regions) were amplified by primer pairs 515 F (GTGCCAGCMGCCGCG GTAA) and 907R (CCGTCAATTCMTTTRAGTTT) (Caporaso et al. 2011; Klindworth et al. 2013). The amplification was carried out with a 50 μL reaction system that contains 25 μl 2× Premix Taq (Takara Biotechnology, Dalian Co. Ltd., China), 1 μL of each primer (10 μM) and 50 ng DNA template. PCR was conducted using the following procedures: thermal cycling conditions were initialized at 95 °C for 2 min, followed by 30 cycles consisting of denaturation at 95 °C for 30 s, annealing at 53 °C for 30 s, and elongation at 72 °C for 30 s, and a final extension at 72 °C for 5 min. The purified PCR amplicon products were subjected to PE250 sequencing on the Illumina platform (Guangdong Magigene Biotechnology Co., Ltd. Guangzhou, China).

Sequencing and bioinformatic analyses

Raw sequence data were quality-filtered using fastp (an ultra-fast all-in-one FASTQ preprocessor, version 0.14.1, https://github.com/OpenGene/fastp). Operational taxonomic units (OTUs) were clustered with a 97% similarity cut-off using UPARSE. The usearch-sintax was used to align the representative sequence of each OTU against the SILVA database for species-level annotation, with a confidence threshold of 0.8. PICRUSt2 (https://github.com/picrust/picrust2) was used to predict the metagenome functions associated with nutrient cycling by performing functional annotation based on KEGG Orthology (KO) numbers, which are used to categorize genes according to their functional roles in metabolic pathways from the Kyoto Encyclopedia of Genes and Genomes (KEGG). The relative abundance of each KO number was calculated by dividing the sums of all KO numbers. The N-cycling processes were calculated by summing the relative abundance of associated KO numbers (Xue et al. 2021). Bacterial OTUs with a

relative abundance of more than 0.5% were chosen to conduct a co-occurrence network based on Spearman correlation analysis ($p < 0.001$, $r > 0.75$). The nutrient-cycling processes were analyzed by determining the relative abundance of genes encoding nutrient-cycling enzymes based on functional prediction for 16S rRNA sequences. The investigated genes encoding N- and P-cycling enzymes can be found in Fig. S1 and Table S1, respectively. The gene abundance representing nutrient-cycling processes was calculated as the sum of genes encoding different enzymes. The abundance of genes encoding the same enzymes were calculated as their average values for N-cycling pathways (Table S1).

The image of the network with the first five modules was generated by Gephi (http://gephi.github.io/). The nodes were clustered using the Louvain algorithm, a modularity optimization-based community detection method, resulting in distinct modules characterized by densely interconnected intra-modular associations and sparsely connected inter-modular linkages (Olesen et al. 2007). Module abundance was calculated by summing the relative abundance of OTUs in the module in bacterial co-occurrence networks. Greater abundance of a module associated with nutrient cycling accounts for greater functional potential of nutrient cycling (Zeng et al. 2024). Module abundance and bacterial diversity were calculated to determine the indirect impacts of plant nutrient-acquisition strategies on nutrient cycling through bacterial abundance within modules.

Analyses of plant nutrient-acquisition strategies and soil properties

We analyzed plant nutrient-acquisition strategies by determining soil pH, leaf manganese concentration ([Mn]) and fine root morphology. The interspecific differences in soil pH were used to represent the ability of plants to acidify soil, as in previous studies (Li et al. 2007; Wen et al. 2020). Soil acidification, caused by proton release, likely drives the carboxylate release from roots due to charge balance (Chai and Schachtman 2022). The pH was measured in a 1:5 (w/v) soil/water suspension (1:2.5 for fine moraine material) using a glass electrode (7252101B) and a potentiometer (pH 6+, EUTECH™, Thermo Fisher Scientific, Waltham, USA). Considering that symbiotic N_2 fixation likely enhances soil acidification through increasing proton release from plant roots and bacterial nitrification and assimilation (Haynes 1983), we measured leaf $\delta^{15}N$ as an indicator of symbiotic N_2 fixation. Leaf $\delta^{15}N$ was determined with an elemental analyzer linked to an isotope ratio mass spectrometer (ISOPRIME 100, Elementar Analysensysteme GmbH, Langenselbold, Germany).

Leaf [Mn] was used to represent the strategy of plant release of carboxylates that mobilize insoluble P (Lambers et al. 2015). The use of mature leaf [Mn] as a proxy for rhizosphere carboxylate concentrations is well documented (Lambers et al. 2015; Zhou et al. 2020, 2021). Plants exhibit high leaf [Mn] as root-released carboxylates enhance the mobilization of soil Mn, which is subsequently absorbed by roots via transporters with low substrate specificity (Lambers et al. 2015, 2021). This proxy has been successfully applied in many field and pot experiments (Teste and Laliberté 2019; Zhong et al. 2021; Zhou et al. 2021; Yan et al. 2024). To determine the role of carboxylate release in solubilization of insoluble soil cations, we measured soil Mn and cation concentrations. The soil cation concentration was calculated as the sum of the concentrations of calcium (Ca), magnesium (Mg) and potassium (K). For the measurement of Mn and cation concentrations, dried leaves were digested with 8 mL nitric acid (68%, w/v) and 2 mL $HClO_4$ (72%, w/v) at 400℃ (Zarcinas et al. 1987). Dried soil was digested with 7 mL nitric acid (68%, w/v) and 3 mL hydrofluoric acid using a microwave digestion system (Nezat et al. 2007). The Mn and cation concentrations in the digested solution of leaves and soil were measured using an atomic absorption spectrometer (ICE™ 3500, Thermo Fisher Scientific, Waltham, US) (Zarcinas et al. 1987).

Specific root length of fine roots is an essential indicator of fine root morphology, representing the capacity of plants to forage soluble nutrients from soil (Lynch 2019). Specific root length was calculated according to the ratio of root length to dry mass (after drying at 70℃). Root length of fine roots was analyzed using WinRHIZO software (Regent, Quebec, Canada) after scanning. Soil nutrient availability is often considered an important factor affecting microbial nutrient cycling through affecting nutrient limitation of soil microorganisms (Zeng et al. 2024). Considering that bioavailable nutrient concentrations (e.g., mineral N and soluble inorganic P) in soil may be a consequence of bacterial nutrient cycling, soil total N and P

concentrations were measured to determine the correlations of nutrient-cycling potential with soil nutrient availability. Soil N concentration was determined with an elemental analyzer (Elementar Vario EL, Elementar Analysensysteme GmbH, Hesse, Germany). The P concentration in the digested solution of soil was determined using a molybdenum-blue method on a microplate reader (SuPerMax 3000 FA, Flash, Shanghai, China) (Murphy and Riley 1962).

Statistics

Linear models were used to determine the interspecific differences in various indicators. To avoid interspecific differences in soil pH being confused with vegetation changes and soil age, linear mixed models were used to determine the correlations among these indicators where successional stages acted as a random effect. Multiple linear regression was used to estimate the effects of plant nutrient-acquisition strategies and soil nutrient concentrations on the abundance of genes encoding nutrient-cycling enzymes. Structural equation models (SEM) were used to assess the mechanisms through which plant P-acquisition strategies were linked to ammonium assimilation and P mobilization. Non-metric multidimensional scaling (NMDS) was used to analyze the module composition. Two axes in NMDS (NMDS 1 and NMDS 2) were used to represent module composition loaded in different dimensions in SEM. The function psem in the R package piecewiseSEM was used to estimate the standardized path coefficients (Lefcheck 2016). Linear models were used to conduct each path in the SEM. For each model, the normality and variance homogeneity of residuals were tested according to histograms of residuals and plots with residuals versus fitted values. The data were transformed and outliers were excluded to normalize the residuals and homogenize the variance of residuals. The Bonferroni adjusted p values were used to determine the significance of models. The R package r.squaredGLMM was used to calculate the marginal R^2 in linear mixed models. All above analyses were performed in R (version 4.1.1). All figures were produced by OriginPro 2024 (Learning Edition).

Results

Differences in plant nutrient-acquisition strategies

Soil pH and SRL served as proxies for plant P-mobilizing and fine root foraging strategies, respectively. The pH at the terminal silts was above 8.5 and significantly higher than that at the S1-S4 stages (Fig. 1a).

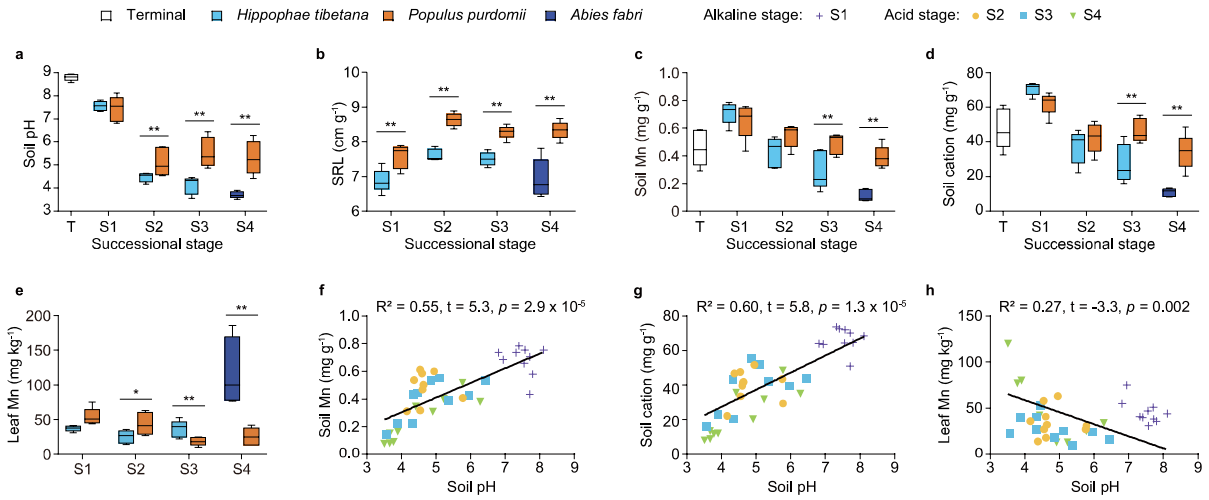


Fig. 1 Plant nutrient-acquisition strategies as dependent on successional stage along the Hailuogou postglacial chronosequence in southwest China. SRL, specific root length; Mn, manganese. Soil cation concentration is the sum of potassium, calcium and magnesium concentrations. In panels **a-e**, linear models were used to determine the interspecific differences (n = 5 for each box). In panels **f–h**, linear mixed models were used to determine the correlations of soil Mn and cation concentrations with soil pH. Asterisks represent significant differences among species (* $p \leq 0.05$, ** $p \leq 0.01$). The boxes show the minimum to maximum values and the lines in the boxes show mean values

At the S2, S3 and S4 stages, soil surrounding *H. tibetana* and *A. fabri* roots exhibited significantly lower pH (Fig. 1a) than that of soil surrounding *P. purdomii*, while *H. tibetana* and *A. fabri* roots exhibited smaller SRL (Fig. 1b). Notably, these acidifying species (*H. tibetana* and *A. fabri*) exhibited significantly lower concentrations of soil Mn and cations (Fig. 1c, d) and higher leaf [Mn] than *P. purdomii* at the S3 and S4 stages (Fig. 1e), despite similar nitrification-related gene abundances among species (Fig. S2a). Soil Mn and cation concentrations (the sum of K, Ca and Mg, Fig. 1d) were significantly and positively correlated with soil pH, while leaf [Mn] showed a negative correlation with soil pH (Fig. 1f-h). In comparison, leaf $\delta^{15}N$ showed an insignificant correlation with soil pH (Fig. S2b).

Differences in bacterial communities in soil surrounding plant roots

We observed significantly lower richness, Shannon index and abundance of genes encoding enzymes involved in denitrification and assimilations of nitrate and ammonium and P mobilization in soil surrounding both *H. tibetana* and *A. fabri* roots compared with soil surrounding *P. purdomii* roots at the S2-S4 stages (Fig. 2a-f). There were no significant differences in bacterial communities at the S1 stage (Fig. 2a-f). Similar to P mobilization, soil surrounding *H. tibetana* and *A. fabri* roots exhibited significantly lower abundance of *gcd*, which is responsible for extracellular carboxylate release from bacteria (Fig. S3a). The gene abundance encoding enzymes involved in ammonium assimilation and P mobilization was an order of magnitude greater than that of genes

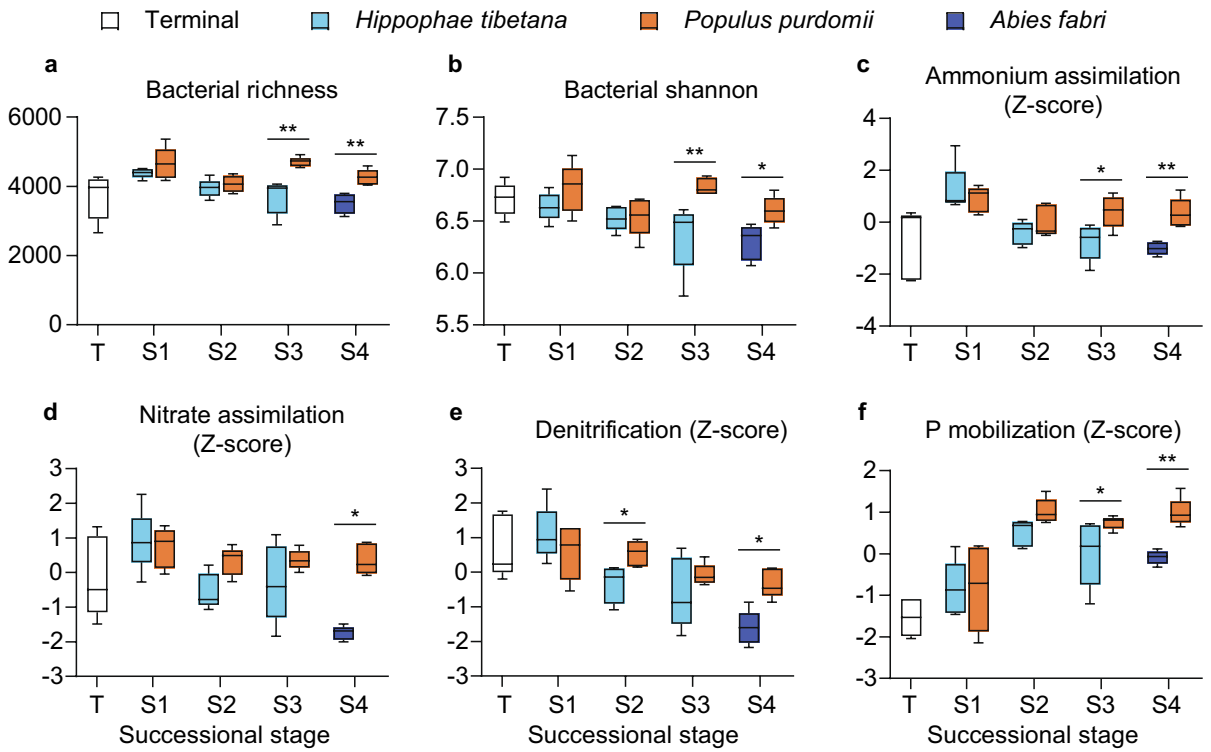


Fig. 2 Differences in bacterial diversity and potential nutrient cycling in soils surrounding roots among plant species along the Hailuogou postglacial chronosequence in southwest China. The normalized gene abundance (Z-score) is shown. T, terminal; S1, S2, S3 and S4 represent stage 1, stage 2, stage 3 and stage 4, respectively. Linear models were used to compare the differences among species at each stage (n = 5 for each box). Asterisks represent significant differences among species (* $p \leq 0.05$, ** $p \leq 0.01$). The boxes show the minimum to maximum values and the lines in the boxes show means

encoding enzymes involved in nitrate assimilation and denitrification (Fig. S3b).

Differences in OTUs among plant species

The bacterial co-occurrence network shows five modules (Fig. 3a). The five modules were ranked according to the taxonomic numbers of OTUs within individual modules, with module 1 exhibiting the greatest taxonomic number but module 5 the lowest (Fig. 3b-f). The most abundant families in modules 1, 2, and 4 were Chitinophagaceae, Burkholderiaceae and Xanthobacteraceae, respectively. Solibacteraceae were the most abundant family in modules 3 and 5. Soil surrounding *H. tibetana* and *A. fabri* roots exhibited significantly greater abundance of modules 2 and 5 but lower abundance of module 4 than that of soil surrounding *P. purdomii* (Fig. 3c, e, f). Such interspecific differences were not significant for modules 1 and 3 (Fig. 3b, d).

The correlations of bacterial communities with plant phosphorus-acquisition strategies and soil nutrient concentrations

Soil surrounding *H. tibetana* and *A. fabri* roots exhibited significantly higher N concentration and lower P concentration than that of soil surrounding *P. purdomii* at the acidic S2-S4 stages (Fig. S4a, b). The potential abundance of genes encoding nutrient-cycling enzymes was more significantly correlated with soil pH and SRL than with soil nutrient concentrations (Table 1). Similarly, the abundance of genes encoding enzymes involved in nitrification showed no significant correlation with soil N concentration (Fig. S4c). The absolute values of standardized regression coefficients for soil pH were significantly greater than those for SRL in linear models (Table 1). The predicted abundance of genes encoding enzymes involved in P mobilization was positively correlated with soil pH at the acidic S2-S4 stages, while the correlation differed at the alkaline S1 stage (Fig. 4a). By contrast, the correlations of the predicted

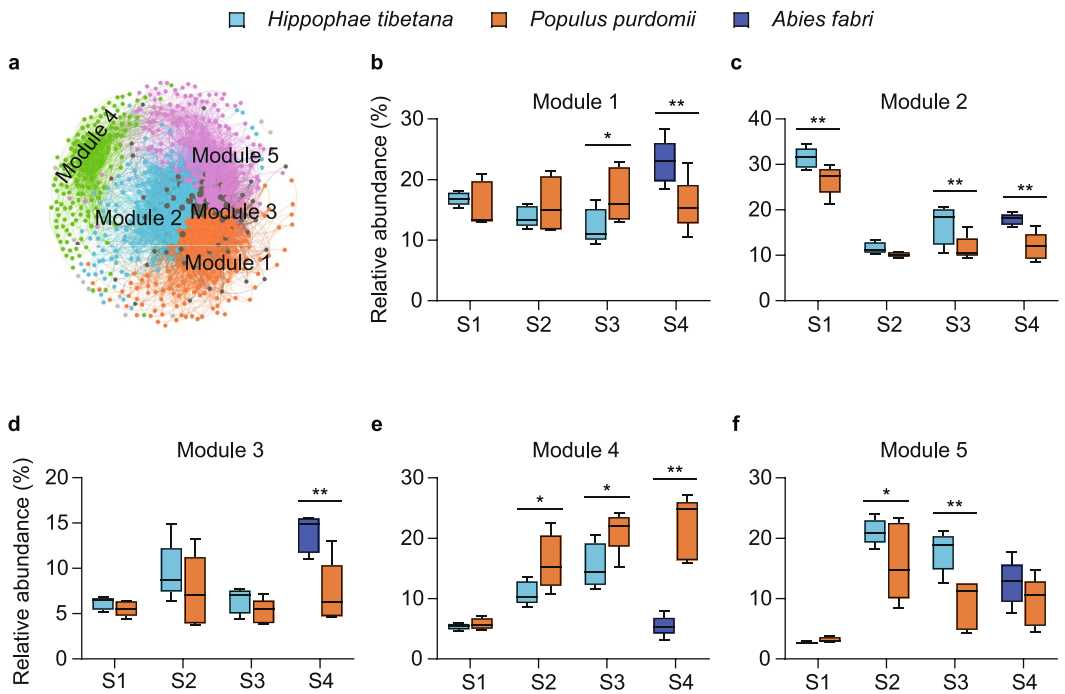


Fig. 3 Module classes in bacterial co-occurrence network in soils surrounding roots among plant species and their variation among successional stages along the Hailuogou postglacial chronosequence in southwest China. S1, S2, S3 and S4 represent stage 1, stage 2, stage 3 and stage 4, respectively. In panel **a**, different modules are filled with different colors. Spearman correlation analysis was used in network analysis (n = 40). Linear models were used to compare the differences among species at each stage (n = 5 for each box). Asterisks represent significant differences among species (* $p \leq 0.05$, ** $p \leq 0.01$). The boxes show the minimum and maximum values and the lines in the boxes show means of relative abundance

Table 1 The correlations of nutrient cycling with plant phosphorus-acquisition strategies and soil nutrient concentrations along the Hailuogou postglacial chronosequence in southwest China

		Explaining variables			
Responsible variables		Soil pH	SRL	Soil P	Soil N
	Model R^2	Coefficients	Coefficients	Coefficients	Coefficients
	F values; *p*	t values; *p*	t values; *p*	t values; *p*	t values; *p*
Phosphorus mobilization	0.43	**− 0.60**** (0.19)	**0.47****(0.13)	0.15 (0.16)	− 0.18 (0.17)
	8.3; 8.1×10^{-5}	− 3.2; 0.003	3.7; 0.001	0.97; 0.339	− 1.0; 0.313
Ammonium assimilation	0.71	**0.78**** (0.14)	0.19 (0.09)	0.12 (0.11)	− 0.02 (0.13)
	23.8; 1.9×10^{-9}	5.7; 2.0×10^{-6}	2.0; 0.051	1.0; 0.309	0.15; 0.886
Nitrate assimilation	0.52	**0.41*** (0.18)	0.18 (0.12)	0.26 (0.14)	− 0.17 (0.16)
	11.5; 4.8×10^{-6}	2.3; 0.026	1.50; 0.134	1.8; 0.085	− 1.1; 0.289
Denitrification	0.49	0.34 (0.18)	0.06 (0.12)	0.20 (0.15)	− 0.31 (0.16)
	10.5; 1.1×10^{-5}	1.9; 0.068	0.48; 0.634	1.4; 0.186	− 0.19; 0.070

Standardized regression coefficients (standard errors) are shown. SRL, specific root length; Soil P, soil total phosphorus concentration; Soil N, Soil total nitrogen concentration. Linear models were used to determine the coefficients and significance. The adjusted R^2 of these models are shown

abundance genes encoding enzymes involved in denitrification and assimilation of nitrate and ammonium N with soil pH was positive at the stages 1–4 (Fig. 4b-d). The decreased bacterial richness and Shannon index and significant change in module abundance were significantly linked to reduced soil pH (Fig. 4e-i).

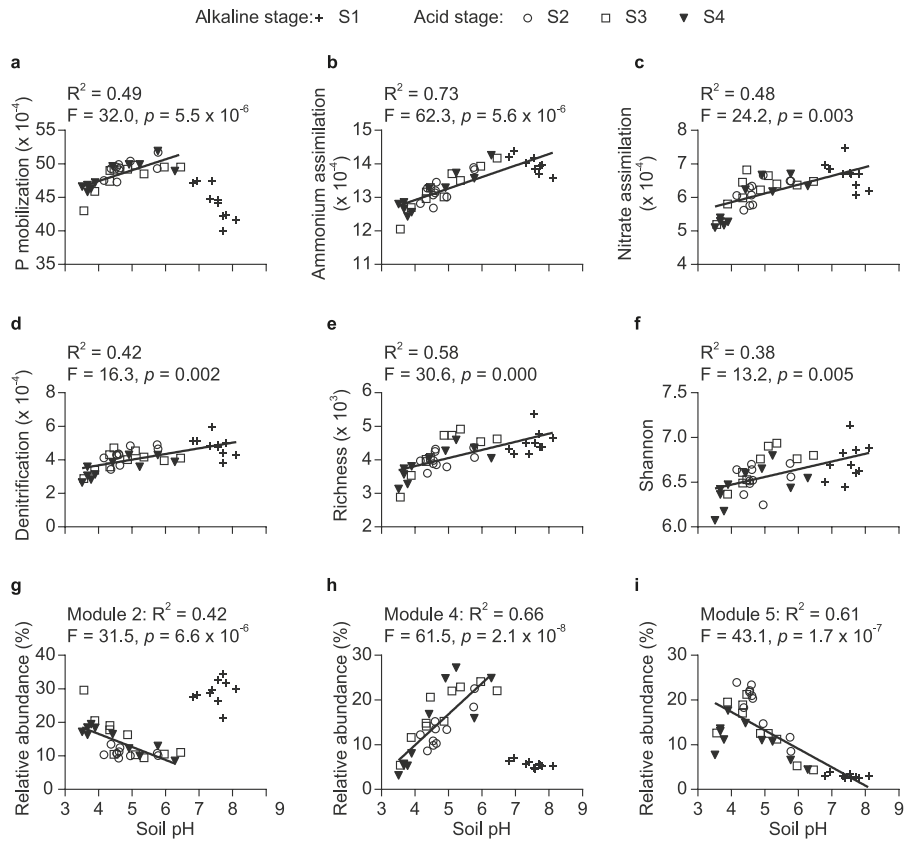


Fig. 4 The correlations of bacterial communities with soil pH in soils surrounding roots of plant species along the Hailuogou postglacial chronosequence in southwest China. S1, S2, S3 and S4 represent stage 1, stage 2, stage 3 and stage 4, respectively. Linear mixed models were used to determine these correlations where successional stages were used as a random effect in each model. In panels **a, h** and **i**, the linear mixed model involved only stages 1–3 because stage 1 exhibited different variation in phosphorus (P) mobilization and module abundance with soil pH compared with stages 1–3

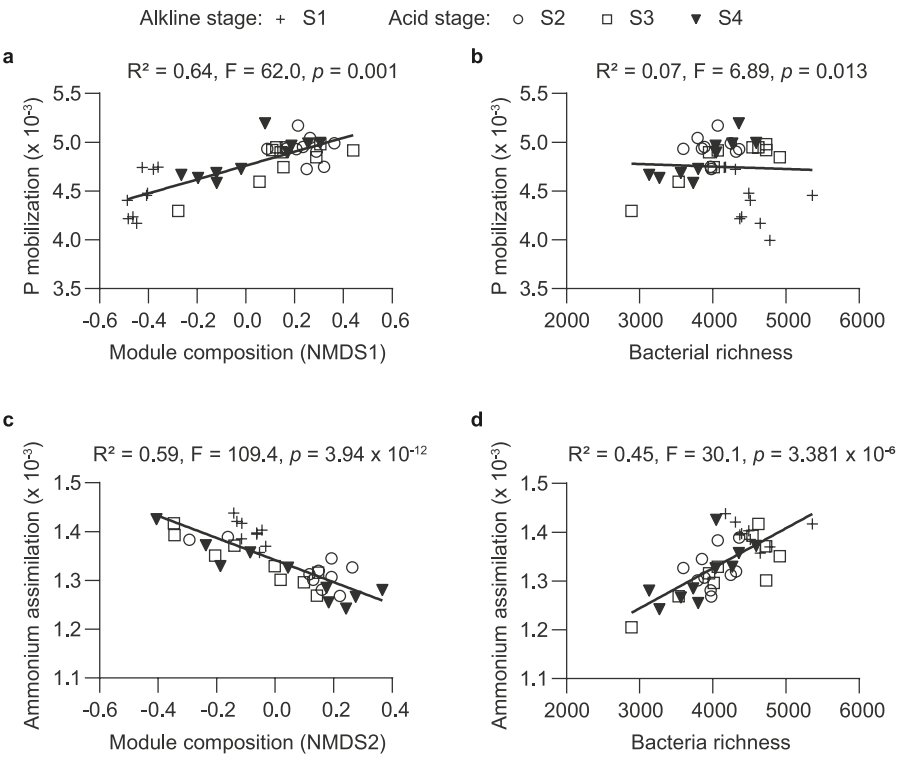


Fig. 5 The correlations of functional abundance of genes encoding nutrient-cycling enzymes with module composition and bacterial richness along the Hailuogou postglacial chronosequence in southwest China. S1, S2, S3 and S4 represent stage 1, stage 2, stage 3 and stage 4, respectively. Linear mixed models were used to determine these correlations. The random effects were successional stages in these mixed models. Non-metric multidimensional scaling (NMDS) was used to analyze the composition of five modules in a co-occurrence network (stress = 0.11). NMDS 1 and NMDS 2 represent the two axes of NMDS and were used to represent module composition loaded in two dimensions

The correlations of abundance of functional genes encoding nutrient-cycling enzymes with module composition and bacterial richness

The predicted abundance of genes encoding enzymes involved in P mobilization and ammonium assimilation was significantly correlated with module composition and bacterial richness, while module composition explained more variance of P mobilization (64% versus 7%) and ammonium assimilation (59% versus 45%) than bacterial richness (Fig. 5a-d).

The direct and indirect correlations of nutrient cycling with plant P-acquisition strategies

Potential pathway analysis showed that the decreased abundance of genes encoding enzymes involved in P mobilization was indirectly associated with the reduced soil pH through the composition of soil bacterial modules (Fig. 6a). In contrast, the abundance of genes encoding enzymes involved in ammonium assimilation was both directly and indirectly associated with the decreased pH, primarily through module composition (Fig. 6b). The abundance of genes encoding enzymes involved in P mobilization or ammonium assimilation showed no significant correlations with bacterial richness (Fig. 6a, b). The pathway coefficients linking soil pH to module composition and bacterial richness were greater than those linking SRL to module composition and bacterial richness (Fig. 6a, b).

Discussion

Rhizosphere acidification was linked to plant P-acquisition strategies rather than bacterial strategies

The differences in soil pH and SRL (Fig. 1a, b) indicate that both *H. tibetana* and *A. fabri* acidified the soil as a strategy for P mobilization, while *P. purdomii* was effective at foraging bioavailable forms of soil nutrients. The acidifying capacity of *H. tibetana* and *A. fabri* is further supported by the loss of Mn and cations in soil surrounding their roots and their significantly positive correlations with soil pH (Fig. 1c, d, f, g). The soils supporting these plants featured relatively homogeneous litter layers and exhibited similar weathering intensity at the same stage (Zhou et al. 2016, 2018). Previous studies conducted

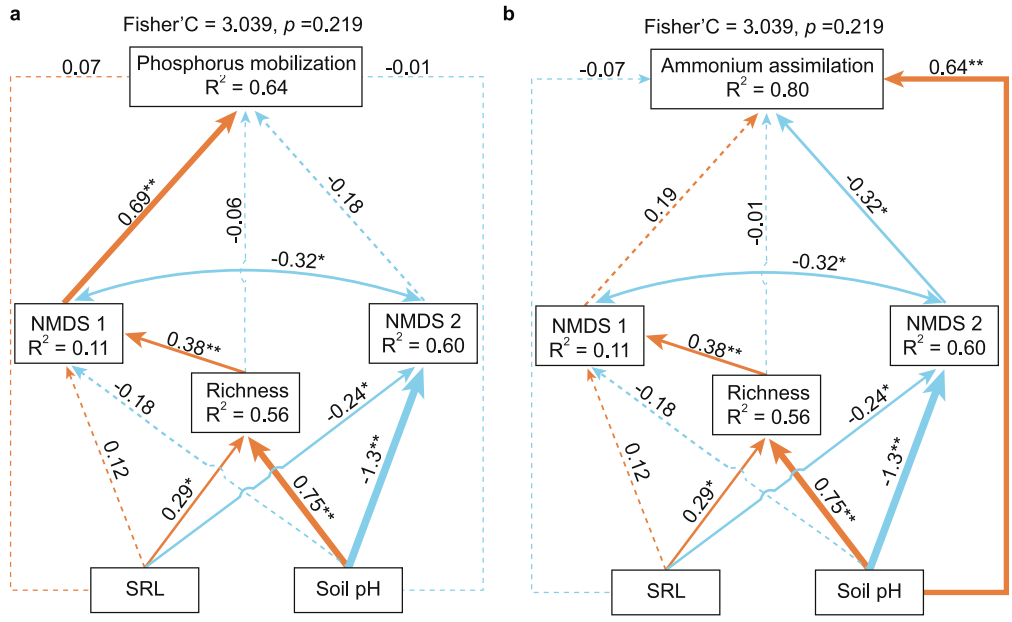


Fig. 6 Potential pathways by which bacterial nitrogen and phosphorus cycling are associated with acidification in soil surrounding plant roots along the Hailuogou postglacial chronosequence in southwest China. The orange and blue arrows represent positive and negative coefficients, respectively. The thicker arrows show greater values of coefficients. Non-metric multidimensional scaling (NMDS) was used to analyze the composition of five modules in a co-occurrence network (stress =0.11). NMDS 1 and NMDS 2 were two axes in NMDS and were used to represent module composition loaded in different dimensions. SRL, specific root length. R package piecewiseSEM was used to determine model validation and parameter (n =39). Linear models were used in each pathway to determine pathway coefficients

along this chronosequence show that soils representing overall communities exhibit small variance in pH at each stage, but soil pH increases with increasing soil depth (Zhou et al. 2016). Considering that roots were concentrated within the topsoil (0–10 cm), the difference in soil pH among species at each stage was mainly caused by plant P acquisition rather than soil weathering and degradation of plant litter. Plant P-acquisition strategies likely contribute to acidification due to the release of protons that drive the release of carboxylates (Chai and Schachtman 2022), as indicated by the negative correlation between leaf [Mn] and soil pH (Fig. 1e). Soil pH was not correlated with leaf $\delta^{15}N$ (Fig. S2), indicating that symbiotic N_2 fixation likely contributed less to soil acidification than carboxylate and proton release. The newly exposed soil exhibited a strong buffering capacity because it contained large amounts of primary minerals that are rich in Ca, K and Mg (Fig. 1b), likely explaining the insignificant interspecific difference in soil pH at the S1 stage.

Although soil nitrifying and P-mobilizing bacteria can contribute to acidification through proton release (Hayat et al. 2010), the lower abundance of genes encoding enzymes involved in P mobilization and nitrification in *H. tibetana* and *A. fabri* soil than in *P. purdomii* soil suggests a limited role of soil bacteria in explaining the interspecific difference in soil pH (Figs. 2f, S2a). Abundant soil ammonium-N is an important factor increasing nitrification by providing substrate and enhancing N availability (Li et al. 2020). Soils conditioned by N_2-fixing plants exhibit greater N concentration and thus greater nitrification rates (Haynes 1983). This was not observed in this study because soil N concentration was not significantly correlated with potential nitrification (Fig. S4c), although *H. tibetana* and *A. fabri* soil exhibited greater soil N concentration than *P. purdomii* soil (Fig. S4a). The rapid increase in soil N concentration (Fig. S4a) likely allowed nitrifying bacteria not to be limited by substrate availability. Also, DeForest and Otuya (2020) found that a decrease in

soil pH from 6.7 to 4.8 slows down nitrification rates by 97%. At the S2–S4 stage, the acid environment (pH = 3.5–6.5) may suppress the activities of nitrifying bacteria, leading to a slow production of protons during nitrification. This is further supported by the decrease in the abundance of genes encoding nitrifying enzymes at the acidic stages compared with the alkaline S2 stage (Fig. S2a).

Phosphate-solubilizing microorganisms likely acidify the soil with protons released to drive the release of carboxylates (Rawat et al. 2021). The *gcd* gene is responsible for the synthesis of enzymes involved in gluconic acid synthesis which is a major acid secreted by bacteria involved in P solubilization (Rodríguez et al. 2006). The significantly lower gene abundance of *gcd* in *H. tibetana* and *A. fabri* soil than in *P. purdomii* soil suggests that P-solubilizing bacteria played a marginal role in lowering soil pH (Fig. S3a). Microbial ammonium assimilation would lead to the secretion of excess protons into soil, thus acidifying soil (Rawat et al. 2021). However, this trait is expressed in alkalophilic *Bacillus marisflavi* FA7 in artificial media, but is not well evidenced in the field in acid soil (Rawat et al. 2021). Carbonic acid generated by microbial respiration also has the potential to decrease soil pH, but soil respiration was largely explained by temperature (59–90%) at each stage along the Hailuogou chronosequence (Luo et al. 2012).

Plant P-mobilizing strategies affect nutrient cycling

Functional genes are frequently considered as biomarkers for predicting specific processes of nutrient cycling (Uroz et al. 2009; Petersen et al. 2012). Mobilizing P and assimilating ammonium by bacteria may be prevalent in soil around plant roots, as gene abundance related to the two processes is an order of magnitude greater than that of other nutrient-transforming processes (Fig. S3b). The differences in the predicted abundance of nutrient-cycling processes among species indicate that the potential P mobilization and ammonium assimilation might be suppressed in *H. tibetana* and *A. fabri* soil compared with that in *P. purdomii* soil at the acidic S2–S4 stages (Fig. 2c-f). This is in line with a previous study that soil dominated by plants with stronger soil acidification exhibit slower microbial nutrient cycling (Bahram et al. 2020).

The nutrient-cycling potential of rhizosphere bacteria was correlated with plant nutrient-acquisition strategies rather than soil nutrient availability, as indicated by the multiple regression models (Table 1). Also, soil acidification might exert greater effects on bacterial ammonium assimilation and P mobilization than fine root foraging did (Fig. 6a, b). Roots take up bioavailable forms of nutrients from soil and decrease substrate availability for soil bacteria (Gutschick 1981), thus likely decreasing the rates of soil nutrient cycling (Moreau et al. 2019). However, the concentrations of bioavailable N and P rapidly increased in acidic soil at the S2–S4 stages during this primary succession (Zhou et al. 2013). The weak impacts of fine root foraging on bacteria may arise from the increased nutrient availability, which can relax the competition for nutrients between roots and surrounding bacteria (Čapek et al. 2018). Also, Wang et al. (2020) found that plants likely do not compete for P with microorganisms since the cycling of soil microbial biomass P is at least an order of magnitude greater than plant P uptake along the Hailuogou chronosequence.

Our results support the contention that the reduced nutrient cycling potential of bacteria was associated with soil acidification (Fig. 4a-d). By incorporating successional stages as a random effect, we were able to isolate the influence of gene abundance and soil pH, ensuring that the observed correlation was not confounded by successional changes (Fig. 4a-d). The negative impact of soil acidification on bacterial nutrient cycling is consistent with previous studies (Fierer and Jackson 2006; Dai et al. 2020). The optimal pH for most microorganisms is near neutral, which is close to their intracellular pH (Madigan et al. 1997). Bacteria generally exhibit low tolerance to a decrease in soil pH (Rousk et al. 2010). Thus, acidification from neutral to acid might decrease bacterial activities and functional potential. In addition, acidification increases the solubilization of soil Mn and aluminum (Lambers et al. 2015, 2022), which may lead to reduced bacterial activities due to toxicity (Kraal et al. 2009; Juttukonda and Skaar 2015). However, the correlation between soil pH and P mobilization varies depending on soil pH, showing distinct differences between acidic and alkaline conditions. Considering the narrow range of pH values (between 6.8 and 8.1) and small sample size at the S1 stage, it is difficult to determine whether potential P mobilization

decreased or simply plateaued with increasing pH in alkaline soil. Zhou et al. (2024) found that fewer bacterial genera tolerate acidic conditions compared with alkaline conditions. This likely explains the different effects of soil pH on P mobilization between acid and alkaline stages.

Our results show that bacterial P mobilization was indirectly and negatively associated with acidification through the bacterial abundance within modules of bacterial networks (Fig. 6a, b). Similarly, Zeng et al. (2024) found that bacterial abundance in a module involved in P cycling account largely for an increase in P-mineralizing potential of bacterial communities when N addition exacerbates bacterial P limitation. The interspecific differences in module abundance and reduced bacterial richness were correlated with soil acidification (Fig. 4e-i), consistent with previous studies (Fierer and Jackson 2006; Zhang et al. 2018). When both module composition and bacterial richness were considered within the same model, module composition was a much more powerful predictor of potential nutrient cycling than bacterial diversity. The significant role of module composition was further supported by the linear mixed models that more variance of nutrient cycling was explained by module composition than by bacterial richness (Fig. 5a-d). Module composition likely features bacterial communities with low functional redundancy because species within individual modules may be involved in similar functions (Olesen et al. 2007). However, species richness is a crude metric in this regard when different taxa support similar nutrient-cycling processes (Wagg et al. 2019).

Implications and limitations

The interactions between plants and soil microorganisms play crucial roles in driving vegetation succession (Reynolds et al. 2003; Kardol et al. 2006; Wubs et al. 2016). Successional predecessors may cause an accumulation of relatively unfavorable rhizosphere microorganisms (e.g., more abundant soil pathogens) than successional successors, leading to species replacement during primary succession (van der Putten et al. 1993; Reynolds et al. 2003). Our findings advance the understanding on how plant-soil interactions drive species replacement. Plant nutrient-acquisition strategies negatively influence rhizosphere bacterial activities and associated nutrient cycling which likely generates negative feedback effects on plant nutrient uptake and growth. Such different accumulation of beneficial microorganisms likely contributes to species replacement.

Soil acidification accompanied by carboxylate release can suppress bacterial degradation of carboxylates. This inhibition enables plants to efficiently acquire sorbed P through their carboxylate-releasing strategy (Weisskopf et al. 2006; Chai and Schachtman 2022). Future studies should investigate potential trade-offs in P-mining strategies between plants and bacteria. For instance, plants with efficient P-mining mechanisms can acquire P independently, potentially suppressing bacterial activity by limiting bacterial access to carboxylates and available P (Weisskopf et al. 2006). Conversely, plants lacking efficient P-mining capabilities may rely on bacterial processes for P mobilization (Jiang et al. 2021).

The significant impacts of plant nutrient-acquisition strategies on bacterial nutrient cycling may not be as significant in non-growing seasons, as low temperature and precipitation are the major factors that limit bacterial activities and associated nutrient cycling (Bahram et al. 2018). It is important to note that our predictions of functional gene abundance were based on bacterial community data rather than quantitative PCR or metagenomic sequencing. Integrating results from both bacterial community composition and absolute gene abundance may provide deeper insights into the interactions between plant and bacterial nutrient-acquisition strategies. Considering that fungi are closely correlated with plant nutrient-acquisition strategies and soil nutrient cycling (Miki et al. 2010; Phillips et al. 2013), future studies may provide a more comprehensive understanding of microbial nutrient cycling through linking fungi and bacteria, as well as root strategies. Additionally, conducting controlled pot experiments that quantify plant nutrient-acquisition strategies, microbial community dynamics, and metagenomic sequencing would be valuable to further elucidate these complex interactions.

Conclusions

This study examined the impact of soil acidification on bacterial nutrient-cycling potential during primary succession along a glacier foreland chronosequence on the eastern edge of the Tibetan Plateau, southwest China.

We found that the reduced N and P cycling potentials of bacteria were linked to soil acidification, which was associated with plant P-acquisition strategies, whereas fine root foraging strategies and variation in soil nutrient status likely had a negligible influence.

The significant shifts in both bacterial diversity and composition of modules within the bacterial co-occurrence network were linked to acidification. Notably, acidification-induced changes in bacterial module abundance likely played a more critical role in influencing nutrient-cycling potential in the rhizosphere than bacterial richness did. These findings address a significant knowledge gap regarding the direct effects of plant P-acquisition strategies on bacterial nutrient cycling, as well as the indirect impacts mediated by bacterial network structures. Furthermore, this study adds a new dimension to our understanding of how plant communities drive changes in belowground bacterial communities and their associated nutrient cycling processes during primary succession and soil formation.

Acknowledgements We sincerely thank the anonymous reviewers for their critical comments, which greatly enhanced the quality of this work.

Author contributions X-L Li and J Zhou contributed to the study conception and design. Material preparation and data collection were performed by X-L Li, H Sun, J Zhou, Y Chen, H-Q Du, Y-X Ming and S Wu. Data analysis was performed by X-L Li. The first draft of the manuscript was written by X-L Li and J Zhou. H Sun, J Zhou and H Lambers commented on and edited previous versions of the manuscript. All authors read and approved the final manuscript.

Funding Open Access funding enabled and organized by CAUL and its Member Institutions. This work was supported by National Natural Science Foundation of China (Grant No. 42477329, 42077005, 42271073 and 42311540015) and Science and Technology Research Program of Institute of Mountain Hazards and Environment, Chinese Academy of Sciences (No. IMHE-ZYTS11). J.Z. was supported by the Sichuan Science and Technology Program (Grant No. 2024YFHZ0178) and the Western China Youth Scholar Program of Chinese Academy of Sciences. H.L. received a support from Deputy Vice Chancellor Research at the University of Western Australia.

Data availability The datasets generated and/or analyzed during the current study are available from the corresponding author on reasonable request.

Declarations

Competing interests Hans Lambers is the Editor-in-Chief of Plant and Soil.

Open Access This article is licensed under a Creative Commons Attribution 4.0 International License, which permits use, sharing, adaptation, distribution and reproduction in any medium or format, as long as you give appropriate credit to the original author(s) and the source, provide a link to the Creative Commons licence, and indicate if changes were made. The images or other third party material in this article are included in the article's Creative Commons licence, unless indicated otherwise in a credit line to the material. If material is not included in the article's Creative Commons licence and your intended use is not permitted by statutory regulation or exceeds the permitted use, you will need to obtain permission directly from the copyright holder. To view a copy of this licence, visit http://creativecommons.org/licenses/by/4.0/.

References

Abalos D, Van Groenigen JW, De Deyn GB (2018) What plant functional traits can reduce nitrous oxide emissions from intensively managed grasslands? Glob Change Biol 24:e248–e258. https://doi.org/10.1111/gcb.13827

Bahram M, Hildebrand F, Forslund SK et al (2018) Structure and function of the global topsoil microbiome. Nature 560:233–237. https://doi.org/10.1038/s41586-018-0386-6

Bahram M, Netherway T, Hildebrand F et al (2020) Plant nutrient-acquisition strategies drive topsoil microbiome structure and function. New Phytol 227:1189–1199. https://doi.org/10.1111/nph.16598

Bai Y, Xiang Q, Zhao K et al (2020) Plant and soil development cooperatively shaped the composition of the *phoD*-harboring bacterial community along the primary succession in the Hailuogou glacier chronosequence. mSystems 5:e00475–20. https://doi.org/10.1128/mSystems.00475-20

Bissett A, Brown MV, Siciliano SD, Thrall PH (2013) Microbial community responses to anthropogenically induced environmental change: towards a systems approach. Ecol Lett 16:128–139. https://doi.org/10.1111/ele.12109

Broadbent FE, Tyler KB (1965) Effect of pH on nitrogen immobilization in two California soils. Plant Soil 23:314–322. https://doi.org/10.1007/BF01347726

Cantarel AAM, Pommier T, Desclos-Theveniau M et al (2015) Using plant traits to explain plant–microbe relationships involved in nitrogen acquisition. Ecology 96:788–799. https://doi.org/10.1890/13-2107.1

Čapek P, Manzoni S, Kaštovská E et al (2018) A plant–microbe interaction framework explaining nutrient effects on primary production. Nat Ecol Evol 2:1588–1596. https://doi.org/10.1038/s41559-018-0662-8

Caporaso JG, Lauber CL, Walters WA et al (2011) Global patterns of 16S rRNA diversity at a depth of millions of sequences per sample. Proc Natl Acad Sci U S A 108:4516–4522. https://doi.org/10.1073/pnas.1000080107

Chai YN, Schachtman DP (2022) Root exudates impact plant performance under abiotic stress. Trends Plant Sci 27:80–91. https://doi.org/10.1016/j.tplants.2021.08.003

Chapman SK, Langley JA, Hart SC, Koch GW (2006) Plants actively control nitrogen cycling: uncorking the microbial bottleneck. New Phytol 169:27–34. https://doi.org/10.1111/j.1469-8137.2005.01571.x

Cheng S, Gong X, Xue W et al (2024) Evolutionarily conserved core microbiota as an extended trait in nitrogen acquisition strategy of herbaceous species. New Phytol 244:1570–1584. https://doi.org/10.1111/nph.20118

Ciccazzo S, Esposito A, Borruso L, Brusetti L (2016) Microbial communities and primary succession in high altitude mountain environments. Ann Microbiol 66:43–60. https://doi.org/10.1007/s13213-015-1130-1

Dai Z, Liu G, Chen H et al (2020) Long-term nutrient inputs shift soil microbial functional profiles of phosphorus cycling in diverse agroecosystems. ISME J 14:757–770. https://doi.org/10.1038/s41396-019-0567-9

DeForest JL, Otuya RK (2020) Soil nitrification increases with elevated phosphorus or soil pH in an acidic mixed mesophytic deciduous forest. Soil Biol Biochem 142:107716. https://doi.org/10.1016/j.soilbio.2020.107716

Elrys AS, Chen Z, Wang J et al (2022) Global patterns of soil gross immobilization of ammonium and nitrate in terrestrial ecosystems. Glob Change Biol 28:4472–4488. https://doi.org/10.1111/gcb.16202

Epihov DZ, Saltonstall K, Batterman SA et al (2021) Legume–microbiome interactions unlock mineral nutrients in regrowing tropical forests. Proc Natl Acad Sci U S A 118:e2022241118. https://doi.org/10.1073/pnas.2022241118

Fan K, Delgado-Baquerizo M, Guo X et al (2021) Biodiversity of key-stone phylotypes determines crop production in a 4-decade fertilization experiment. ISME J 15:550–561. https://doi.org/10.1038/s41396-020-00796-8

Fierer N, Jackson RB (2006) The diversity and biogeography of soil bacterial communities. Proc Natl Acad Sci U S A 103:626–631. https://doi.org/10.1073/pnas.0507535103

Fisher KA, Yarwood SA, James BR (2017) Soil urease activity and bacterial ureC gene copy numbers: effect of pH. Geoderma 285:1–8. https://doi.org/10.1016/j.geoderma.2016.09.012

Francis R, Read DJ (1994) The contributions of mycorrhizal fungi to the determination of plant community structure. Plant Soil 159:11–25. https://doi.org/10.1007/BF00000091

Gutschick VP (1981) Evolved strategies in nitrogen acquisition by plants. Am Nat 118:607–637. https://doi.org/10.1086/283858

Hayat R, Ali S, Amara U et al (2010) Soil beneficial bacteria and their role in plant growth promotion: a review. Ann Microbiol 60:579–598. https://doi.org/10.1007/s13213-010-0117-1

Haynes RJ (1983) Soil acidification induced by leguminous crops. Grass Forage Sci 38:1–11. https://doi.org/10.1111/j.1365-2494.1983.tb01614.x

Henneron L, Kardol P, Wardle DA et al (2020) Rhizosphere control of soil nitrogen cycling: a key component of plant economic strategies. New Phytol 228:1269–1282. https://doi.org/10.1111/nph.16760

Hu Z, Delgado-Baquerizo M, Fanin N et al (2024) Nutrient-induced acidification modulates soil biodiversity-function relationships. Nat Commun 15:2858. https://doi.org/10.1038/s41467-024-47323-3

Jiang F, Zhang L, Zhou J et al (2021) Arbuscular mycorrhizal fungi enhance mineralisation of organic phosphorus by carrying bacteria along their extraradical hyphae. New Phytol 230:304–315. https://doi.org/10.1111/nph.17081

Juttukonda LJ, Skaar EP (2015) Manganese homeostasis and utilization in pathogenic bacteria. Mol Microbiol 97:216–228. https://doi.org/10.1111/mmi.13034

Kardol P, Martijn Bezemer T, van der Putten WH (2006) Temporal variation in plant–soil feedback controls succession. Ecol Lett 9:1080–1088. https://doi.org/10.1111/j.1461-0248.2006.00953.x

Klindworth A, Pruesse E, Schweer T et al (2013) Evaluation of general 16S ribosomal RNA gene PCR primers for classical and next-generation sequencing-based diversity studies. Nucleic Acids Res 41:e1. https://doi.org/10.1093/nar/gks808

Kraal P, Nierop KGJ, Kaal J, Tietema A (2009) Carbon respiration and nitrogen dynamics in Corsican pine litter amended with aluminium and tannins. Soil Biol Biochem 41:2318–2327. https://doi.org/10.1016/j.soilbio.2009.08.017

Kuypers MMM, Marchant HK, Kartal B (2018) The microbial nitrogen-cycling network. Nat Rev Microbiol 16:263–276. https://doi.org/10.1038/nrmicro.2018.9

Kuzyakov Y, Xu X (2013) Competition between roots and microorganisms for nitrogen: mechanisms and ecological relevance. New Phytol 198:656–669. https://doi.org/10.1111/nph.12235

Lambers H (2022) Phosphorus acquisition and utilization in plants. Annu Rev Plant Biol 73:17–42. https://doi.org/10.1146/annurev-arplant-102720-125738

Lambers H, Raven J, Shaver G, Smith S (2008) Plant nutrient-acquisition strategies change with soil age. Trends Ecol Evol 23:95–103. https://doi.org/10.1016/j.tree.2007.10.008

Lambers H, Hayes PE, Laliberté E et al (2015) Leaf manganese accumulation and phosphorus-acquisition efficiency. Trends Plant Sci 20:83–90. https://doi.org/10.1016/j.tplants.2014.10.007

Lambers H, Wright IJ, Guilherme Pereira C et al (2021) Leaf manganese concentrations as a tool to assess belowground plant functioning in phosphorus-impoverished environments. Plant Soil 461:43–61. https://doi.org/10.1007/s11104-020-04690-2

Lambers H, De Britto CP, Cawthray GR et al (2022) Strategies to acquire and use phosphorus in phosphorus-impoverished and fire-prone environments. Plant Soil 476:133–160. https://doi.org/10.1007/s11104-022-05464-8

Lefcheck JS (2016) piecewiseSEM: piecewise structural equation modelling in r for ecology, evolution, and systematics. Methods Ecol Evol 7:573–579. https://doi.org/10.1111/2041-210X.12512

Li X, Xiong S (1995) Vegetation primary succession on glacier foreland in Hailuogou. Mt. Gongga. Mt Res 13:109–115. https://doi.org/10.16089/j.cnki.1008-2786.1995.02.008

Li L, Li S-M, Sun J-H et al (2007) Diversity enhances agricultural productivity via rhizosphere phosphorus facilitation

on phosphorus-deficient soils. Proc Natl Acad Sci U S A 104:11192–11196. https://doi.org/10.1073/pnas.0704591104

Li Z, Zeng Z, Tian D et al (2020) Global patterns and controlling factors of soil nitrification rate. Glob Change Biol 26:4147–4157. https://doi.org/10.1111/gcb.15119

Li X-L, Zhou J, Du H-Q et al (2025) Plant nutrient-acquisition strategies contribute to species replacement during primary succession. J Ecol 113:988–1003. https://doi.org/10.1111/1365-2745.70017

Luo J, Chen Y, Wu Y et al (2012) Temporal-spatial variation and controls of soil respiration in different primary succession stages on glacier forehead in Gongga Mountain. China PLoS One 7:e42354. https://doi.org/10.1371/journal.pone.0042354

Lynch JP (2019) Root phenotypes for improved nutrient capture: an underexploited opportunity for global agriculture. New Phytol 223:548–564. https://doi.org/10.1111/nph.15738

Madigan MT, Martinko JM, Parker J (1997) Brock biology of microorganisms. Prentice Hall, Upper Saddle River, New Jersey

McGrath JW, Chin JP, Quinn JP (2013) Organophosphonates revealed: new insights into the microbial metabolism of ancient molecules. Nat Rev Microbiol 11:412–419. https://doi.org/10.1038/nrmicro3011

Miki T, Ushio M, Fukui S, Kondoh M (2010) Functional diversity of microbial decomposers facilitates plant coexistence in a plant–microbe–soil feedback model. Proc Natl Acad Sci U S A 107:14251–14256. https://doi.org/10.1073/pnas.0914281107

Moreau D, Bardgett RD, Finlay RD et al (2019) A plant perspective on nitrogen cycling in the rhizosphere. Funct Ecol 33:540–552. https://doi.org/10.1111/1365-2435.13303

Murphy J, Riley JP (1962) A modified single solution method for the determination of phosphate in natural waters. Anal Chim Acta 27:31–36. https://doi.org/10.1016/S0003-2670(00)88444-5

Nezat CA, Blum JD, Yanai RD, Hamburg SP (2007) A sequential extraction to determine the distribution of apatite in granitoid soil mineral pools with application to weathering at the Hubbard Brook Experimental Forest, NH, USA. Appl Geochem 22:2406–2421. https://doi.org/10.1016/j.apgeochem.2007.06.012

Olesen JM, Bascompte J, Dupont YL, Jordano P (2007) The modularity of pollination networks. Proc Natl Acad Sci U S A 104:19891–19896. https://doi.org/10.1073/pnas.0706375104

Ortiz-Álvarez R, Fierer N, De Los RA et al (2018) Consistent changes in the taxonomic structure and functional attributes of bacterial communities during primary succession. ISME J 12:1658–1667. https://doi.org/10.1038/s41396-018-0076-2

Perakis SS, Pett-Ridge JC (2019) Nitrogen-fixing red alder trees tap rock-derived nutrients. Proc Natl Acad Sci U S A 116:5009–5014. https://doi.org/10.1073/pnas.1814782116

Petersen DG, Blazewicz SJ, Firestone M et al (2012) Abundance of microbial genes associated with nitrogen cycling as indices of biogeochemical process rates across a vegetation gradient in Alaska. Environ Microbiol 14:993–1008. https://doi.org/10.1111/j.1462-2920.2011.02679.x

Philippot L, Spor A, Hénault C et al (2013) Loss in microbial diversity affects nitrogen cycling in soil. ISME J 7:1609–1619. https://doi.org/10.1038/ismej.2013.34

Phillips RP, Brzostek E, Midgley MG (2013) The mycorrhizal-associated nutrient economy: a new framework for predicting carbon–nutrient couplings in temperate forests. New Phytol 199:41–51. https://doi.org/10.1111/nph.12221

Prescott CE, Grayston SJ, Helmisaari H-S et al (2020) Surplus carbon drives allocation and plant–soil interactions. Trends Ecol Evol 35:1110–1118. https://doi.org/10.1016/j.tree.2020.08.007

Rawat P, Das S, Shankhdhar D, Shankhdhar SC (2021) Phosphate-solubilizing microorganisms: mechanism and their role in phosphate solubilization and uptake. J Soil Sci Plant Nutr 21:49–68. https://doi.org/10.1007/s42729-020-00342-7

Reynolds HL, Packer A, Bever JD, Clay K (2003) Grassroots ecology: plant–microbe–soil interactions as drivers of plant community structure and dynamics. Ecology 84:2281–2291. https://doi.org/10.1890/02-0298

Rodríguez H, Fraga R, Gonzalez T, Bashan Y (2006) Genetics of phosphate solubilization and its potential applications for improving plant growth-promoting bacteria. Plant Soil 287:15–21. https://doi.org/10.1007/s11104-006-9056-9

Rousk J, Bååth E, Brookes PC et al (2010) Soil bacterial and fungal communities across a pH gradient in an arable soil. ISME J 4:1340–1351. https://doi.org/10.1038/ismej.2010.58

Shah SRU, Agback P, Lundquist P-O (2015) Root morphology and cluster root formation by seabuckthorn (*Hippophaë rhamnoides* L.) in response to nitrogen, phosphorus and iron deficiency. Plant Soil 397:75–91. https://doi.org/10.1007/s11104-015-2598-y

Sparrius LB, Kooijman AM (2013) Nitrogen deposition and soil carbon content affect nitrogen mineralization during primary succession in acid inland drift sand vegetation. Plant Soil 364:219–228. https://doi.org/10.1007/s11104-012-1351-z

Sun S, Ma B, Wang G, Tan X (2023) Linking microbial biogeochemical cycling genes to the rhizosphere of pioneering plants in a glacier foreland. Sci Total Environ 872:161944. https://doi.org/10.1016/j.scitotenv.2023.161944

Teste FP, Laliberté E (2019) Plasticity in root symbioses following shifts in soil nutrient availability during long-term ecosystem development. J Ecol 107:633–649. https://doi.org/10.1111/1365-2745.13103

Turner S, Mikutta R, Guggenberger G et al (2019) Distinct pattern of nitrogen functional gene abundances in top- and subsoils along a 120,000-year ecosystem development gradient. Soil Biol Biochem 132:111–119. https://doi.org/10.1016/j.soilbio.2019.02.006

Uroz S, Calvaruso C, Turpault M-P, Frey-Klett P (2009) Mineral weathering by bacteria: ecology, actors and mechanisms. Trends Microbiol 17:378–387. https://doi.org/10.1016/j.tim.2009.05.004

van der Putten WH, Van Dijk C, Peters BAM (1993) Plant-specific soil-borne diseases contribute to succession in

foredune vegetation. Nature 362:53–56. https://doi.org/10.1038/362053a0
Wagg C, Schlaeppi K, Banerjee S et al (2019) Fungal-bacterial diversity and microbiome complexity predict ecosystem functioning. Nat Commun 10:4841. https://doi.org/10.1038/s41467-019-12798-y
Wang J, Wu Y, Zhou J et al (2020) Soil microbes become a major pool of biological phosphorus during the early stage of soil development with little evidence of competition for phosphorus with plants. Plant Soil 446:259–274. https://doi.org/10.1007/s11104-019-04329-x
Wassen MJ, Venterink HO, Lapshina ED, Tanneberger F (2005) Endangered plants persist under phosphorus limitation. Nature 437:547–550. https://doi.org/10.1038/nature03950
Weisskopf L, Abou-Mansour E, Fromin N et al (2006) White lupin has developed a complex strategy to limit microbial degradation of secreted citrate required for phosphate acquisition. Plant Cell Environ 29:919–927. https://doi.org/10.1111/j.1365-3040.2005.01473.x
Wen Z, Pang J, Tueux G et al (2020) Contrasting patterns in biomass allocation, root morphology and mycorrhizal symbiosis for phosphorus acquisition among 20 chickpea genotypes with different amounts of rhizosheath carboxylates. Funct Ecol 34:1311–1324. https://doi.org/10.1111/1365-2435.13562
Wubs ERJ, van der Putten WH, Bosch M, Bezemer TM (2016) Soil inoculation steers restoration of terrestrial ecosystems. Nat Plants 2:16107. https://doi.org/10.1038/nplants.2016.107
Xia Z, He Y, Yu L et al (2020a) Sex-specific strategies of phosphorus (P) acquisition in *Populus cathayana* as affected by soil P availability and distribution. New Phytol 225:782–792. https://doi.org/10.1111/nph.16170
Xia Z, He Y, Yu L et al (2020b) Root traits and rhizosphere processes reflect differential phosphorus acquisition strategies in contrasting *Populus* clones. For Ecol Manage 457:117750. https://doi.org/10.1016/j.foreco.2019.117750
Xue C-X, Lin H, Zhu X-Y et al (2021) DiTing: a pipeline to infer and compare biogeochemical pathways from metagenomic and metatranscriptomic data. Front Microbiol 12:698286. https://doi.org/10.3389/fmicb.2021.698286
Yan L, Tang D, Pang J, Lambers H (2024) Root carboxylate release is common in phosphorus-limited forest ecosystems in China: using leaf manganese concentration as a proxy. Plant Soil. https://doi.org/10.1007/s11104-024-06791-8
Zarcinas BA, Cartwright B, Spouncer LR (1987) Nitric acid digestion and multi-element analysis of plant material by inductively coupled plasma spectrometry. Commun Soil Sci Plant Anal 18:131–146. https://doi.org/10.1080/00103628709367806
Zemunik G, Turner BL, Lambers H, Laliberté E (2015) Diversity of plant nutrient-acquisition strategies increases during long-term ecosystem development. Nat Plants 1:15050. https://doi.org/10.1038/nplants.2015.50
Zeng Q, Peñuelas J, Sardans J et al (2024) Keystone bacterial functional module activates P-mineralizing genes to enhance enzymatic hydrolysis of organic P in a subtropical forest soil with 5-year N addition. Soil Biol Biochem 192:109383. https://doi.org/10.1016/j.soilbio.2024.109383
Zhang B, Zhang J, Liu Y et al (2018) Co-occurrence patterns of soybean rhizosphere microbiome at a continental scale. Soil Biol Biochem 118:178–186. https://doi.org/10.1016/j.soilbio.2017.12.011
Zhong H, Zhou J, Azmi A et al (2021) *Xylomelum occidentale* (Proteaceae) accesses relatively mobile soil organic phosphorus without releasing carboxylates. J Ecol 109:246–259. https://doi.org/10.1111/1365-2745.13468
Zhou J, Wu Y, Prietzel J et al (2013) Changes of soil phosphorus speciation along a 120-year soil chronosequence in the Hailuogou glacier retreat area (Gongga Mountain, SW China). Geoderma 195–196:251–259. https://doi.org/10.1016/j.geoderma.2012.12.010
Zhou J, Bing H, Wu Y et al (2016) Rapid weathering processes of a 120-year-old chronosequence in the Hailuogou glacier foreland, Mt. Gongga. SW China Geoderma 267:78–91. https://doi.org/10.1016/j.geoderma.2015.12.024
Zhou J, Bing H, Wu Y et al (2018) Weathering of primary mineral phosphate in the early stages of ecosystem development in the Hailuogou glacier foreland chronosequence. Eur J Soil Sci 69:450–461. https://doi.org/10.1111/ejss.12536
Zhou J, Wu Y, Turner BL et al (2019) Transformation of soil organic phosphorus along the Hailuogou post-glacial chronosequence, southeastern edge of the Tibetan Plateau. Geoderma 352:414–421. https://doi.org/10.1016/j.geoderma.2019.05.038
Zhou J, Zúñiga-Feest A, Lambers H (2020) In the beginning, there was only bare regolith—then some plants arrived and changed the regolith. J Plant Ecol 13:511–516. https://doi.org/10.1093/jpe/rtaa030
Zhou J, Li X, Peng F et al (2021) Mobilization of soil phosphate after 8 years of warming is linked to plant phosphorus-acquisition strategies in an alpine meadow on the Qinghai-Tibetan Plateau. Global Change Biol 27:6578–6591. https://doi.org/10.1111/gcb.15914
Zhou J, Zheng Y, Hou L et al (2023) Effects of acidification on nitrification and associated nitrous oxide emission in estuarine and coastal waters. Nat Commun 14:1380. https://doi.org/10.1038/s41467-023-37104-9
Zhou X, Tahvanainen T, Malard L et al (2024) Global analysis of soil bacterial genera and diversity in response to pH. Soil Biol Biochem 198:109552. https://doi.org/10.1016/j.soilbio.2024.109552

Publisher's Note Springer Nature remains neutral with regard to jurisdictional claims in published maps and institutional affiliations.